Katholieke Universiteit Leuven

Department of Electrical Engineering

ESAT-SISTA/TR 1993-36

A mechatronics approach to electronic control of continuously variable transmissions: towards the limits of performance of combustion engine cars[1]

Paul Vanvuchelen[2], Bart De Moor[3] and Dirk Reniers[4]

July 1993
Submitted for publication in
IEEE Transactions on Control Systems Technology,
Special Issue on Automotive Control Systems

[1]This report is available by anonymous ftp from *gate.esat.kuleuven.ac.be* in the directory *pub/SISTA/vanvuche/reports/cvtelec.ps.Z*

[2]ESAT - Katholieke Universiteit Leuven, Kardinaal Mercierlaan 94, 3001 Leuven (Heverlee), Belgium, tel 32/16/22 09 31, fax 32/16/22 18 55, email: *paul.vanvuchelen@esat.kuleuven.ac.be* and *bart.demoor@esat.kuleuven.ac.be*. This research was sponsored by the Flemish Institute for Scientific and Technological Research in Industry (I.W.T.) and the Belgian programme on Interuniversity Attraction Poles (IUAP-50) initiated by the Belgian State - Prime Minister's Office - Science Policy Programming. The scientific responsibility is assumed by its authors.

[3]Bart De Moor is a research associate with the N.F.W.O. (Belgian National Fund for Scientific Research).

[4]VCST Variable Transmission N.V., Groenstraat 60, 3800 Sint-Truiden, Belgium, tel 32/11/67 02 11, fax 32/11/67 33 27.

Abstract

The technology of a Continuously Variable Transmission (CVT) has been around for many years now. While its reliability, durability, efficiency and controllability have been problems in the past, all but controllability have been greatly improved recently. This paper outlines a possible approach for electronic control of a mechanical CVT that consists of a wet multi-plate clutch and a pushbelt variator. Using a mechatronics approach, the ultimate powertrain control problem (optimal shifting) is translated in a set of hierarchical control problems. To solve these, a model based control design approach is used.

Initially, at the powertrain level, the system components are assumed to be ideal. Bond graph modeling is used to derive the physical model. To realize optimal shifting, the concept of variogram control is introduced, which is then implemented by designing two PI-controllers. Next, at the powertrain component level, the characteristics of the variator and the clutch are taken into account. Although an explicit static feedforward is obtained from the static equilibria, PI-controllers are added, to deal with modeling errors and uncertainty. Finally, the behavior of the electro-hydraulic actuator is investigated. Physical models of the servo valves are constructed with bond graphs and can be used to do prototyping. To robustify the design, further reduction of the actuator influence is done by adding actuator control. Linear models, obtained from black-box identification, are used to design gain scheduled PI-controllers. Validation on the physical models shows that the final influence of the actuator becomes very small.

Besides results on control design, several results on modeling and identification are presented and discussed as well.

I. INTRODUCTION

Ever since in June 1988 a report on global warming was published by the National Academy of Science (NAS), it has become an urgent task to restrict fuel consumption and to decrease CO_2 exhausted from cars. In addition, safety and comfort are important themes in the overall improvement of automobiles. Because all of these themes are significantly affected by the powertrain, powertrain control will play a very important role in the future. In this context, the continuously variable transmission (CVT) will have a great potential. For all of the above mentioned, the importance of electronic control is growing steadily [12].
A schematic representation of the powertrain in combustion engine cars is given in figure 1. The technology of the subsystems and the degree of automation in powertrain control are mainly determined by the type of transmission.

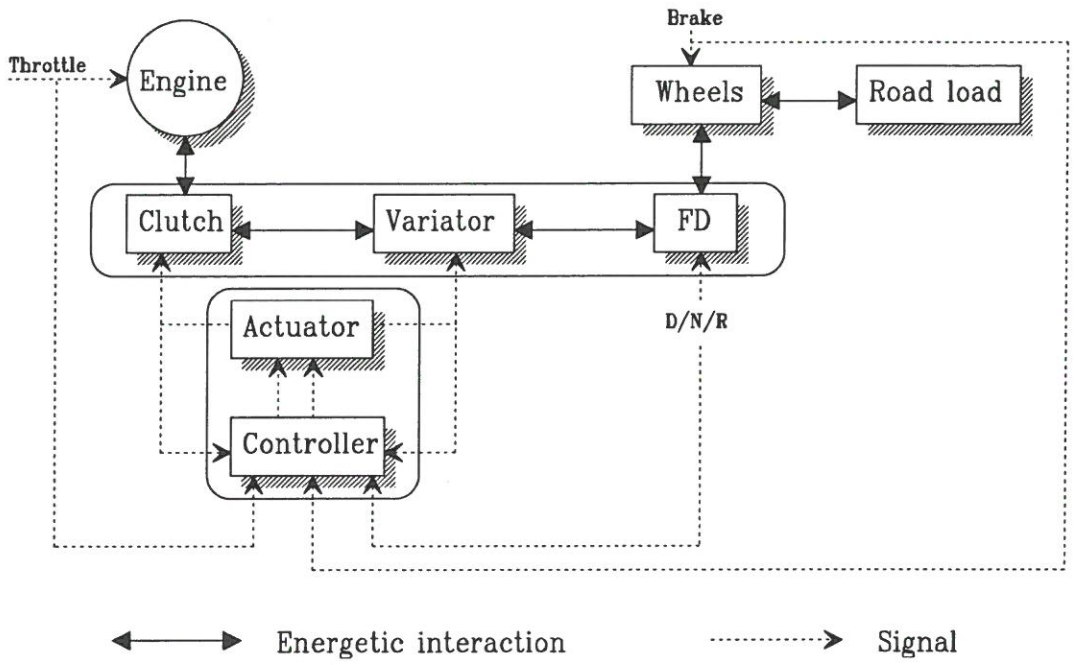


Figure 1: *A schematic representation of the powertrain in combustion engine cars. The engine power is transmitted to the wheels, by a clutch, a variator and a final drive reduction (FD). The essential inputs from the driver are the throttle position, the drive-sense (D(rive), N(eutral), R(everse)) and the brake action. The clutch and the variator are driven by an actuator, which translates the intended control actions into appropriate servo actions.*

In a traditional 5-speed manual transmission (MT), a dry friction clutch and a gear box with 5 fixed ratios are used, respectively as clutch and as variator. The actuator exists of the

clutch pedal, the poker and some mechanical components. Since the driver interacts directly via the actuator, all actions are controlled by the driver. Hence, the degree of automation in powertrain control is negligible.
The degree of automation is necessarily higher in a 5-speed automatic transmission (AT). Often, a torque converter with lock-up facilities is used as clutch, while planetary gears with 5 fixed ratios serve as variator. The actuator and the controller are implemented together, using hydraulic servo valves and specific mechanical components. Although the level of automation is high, this type of control is far from optimal, because the control intelligence is limited, since it must be representable in hardware. However, there's a tendency in AT-control to replace mechanical and hydraulical components by electronic control. In Chrysler's A-604 AT, this is done to obtain a higher drive comfort, a substantial simplification and weight reduction of the mechanism and to reduce the cost [7].
However, due to its original concept, a CVT might have greatest potential for automated powertrain control. In a CVT, shifting between fixed ratios (as in an MT or AT) is replaced by continuous variation between an infinite number of ratios, where the width of variation is determined by the chosen variator type and its construction. Although electrical (hybrid cars) and hydraulical variators exist, mechanical variators are preferred because of their higher efficiency [14]. However, from comfort and driveability considerations, a clutch is still required. Typical clutches are an electromagnetic powder clutch, a wet multi-plate clutch or a torque converter.

A CVT is an intrinsic automatic transmission, which implies that the system only operates well if it is fully automated. The type of clutch control depends on the used clutch: the electromagnetic powderclutch in Subaru's ECVT is electronically controlled, while the wet multi-plate clutch in the VT-1 of the Belgian firm VCST is hydraulically controlled. However, the ratio change of the mechanical variators is still controlled using hydraulic servo valves and specific mechanical components. In the future, it is absolutely necessary to extensively utilize computer control, to optimize the excellent characteristics of CVT's [12].

In this paper, we present a mechatronics approach for electronic control of a CVT with a wet multi-plate clutch and a pushbelt variator. A topdown approach is used to translate the powertrain control problem into a set of hierarchically related subproblems. Bond graph modeling, static modeling and linear identification are used to obtain models of the powertrain, the wet multi-plate clutch, the pushbelt variator and the electro-hydraulic actuator. Once the static and/or dynamic behavior of all components and their interactions are modelled, these

models are implemented in Matrix$_X$ [10]. Based on these models, Computer Aided Control System Design (CACSD) methods are used to design controllers for all subsystems.

Major design advantages of our approach are:

- The proposed control strategy is fairly general and can easily be adapted to each car/engine combination that contains a CVT.
- The topdown approach leads to a controller with an hierarchical structure, where each subcontroller controls a specific subsystem. This implies that if the parameters of a certain subsystem are changed, only the corresponding subcontroller must be changed.
- Compared to the classical prototyping methods, our model based controller design method is cheaper and faster, so more alternatives can be evaluated, for lower cost.
- Unlike the classical mechanical and hydraulical control systems, our control parameters can be changed fast and for lower cost.

Besides substantial design advantages, our approach also leads to an increase in performance of the powertrain and its subsystems:

- Variogram control makes it possible to implement an optimal drive-concept, which permits to approach the limits of performance of combustion engine cars.
- Due to computer control, a throttle dependent stall rotation speed can be implemented, which permits to realize a smooth and fast drive away behavior. Such a stall behavior is not possible when a simple hydraulical control system is used.
- Taking into account the highly non-linear characteristics of the variator and the clutch, the implemented controller will be less conservative then the classical hardware controllers.
- The implementation of actuator control drastically reduces the influence of the oil temperature and the engine rotation speed on the behavior of the electro-hydraulic actuator.

This paper is organized as follows: in section II, two optimal drive-concepts are presented: sport mode is optimal with respect to the delivered engine power, while economy mode is optimal with respect to fuel consumption. To realize an optimal drive-concept, the idea of variogram control is introduced in section III. In this section, a car with ideal powertrain

components is analyzed and controlled. The clutch is treated as an ideal modulated friction element, while the variator is seen as an ideal modulated power transformer. Next, in section IV, it is shown how the characteristics of the wet multi-plate clutch and the pushbelt variator are determined and can be taken into account. In section V, physical models of the electro-hydraulic actuator are derived, to study the influence of the actuator on the powertrain control loop. To minimize the influence of the oil temperature and the engine speed on the actuator characteristics, a gain scheduled PI-controller is derived. Finally, in section VI, the different controllers are combined in a single controller with an hierarchical structure. Closed-loop simulations demonstrate that the proposed algorithm works efficiently. For the sake of completeness, two appendices are added. Appendix A explains the details of the software implementation, while appendix B contains a list of the most important notations that are used through the paper.

II. OPTIMAL DRIVE-CONCEPTS

Before going into details on powertrain control, some notes on combustion engine management are necessary. In [14], a drive-concept is called ideal, if the engine power P_e is a function of the throttle position α only, being independent of the engine rotation speed N_e:

$$P_e = c(\alpha) \tag{1}$$

Because it holds that $P_e = \frac{2\pi}{60} T_e N_e$, the ideal engine torque T_e is given by:

$$T_e = \frac{60\ c(\alpha)}{2\pi N_e} \tag{2}$$

However, the torque-speed characteristic of a combustion engine is far from ideal: the power source has torque-speed curves, which are not hyperbolae as in (2). Due to this deviation between the ideal and the real characteristic, it is necessary to provide a torque-speed transformer (a transmission) between the engine and the wheels.

In practice, combustion engines are characterized by two curves. The torque-speed characteristic relates the delivered engine torque T_e to the engine rotation speed N_e and the throttle position α (see figure 2), while the BSFC diagram, better known as the egg-diagram, represents the brake specific fuel consumption b_e as a function of the engine rotation speed N_e and the delivered engine torque T_e (see figure 3).

For a given transmission ratio $i = N_e/N_w$ (N_w is the wheel rotation speed), the driving torque T_w and the driving power P_w at the wheels are computed as:

$$T_w = iT_e\eta_d \quad (3)$$

$$P_w = \frac{2\pi}{60}T_wN_w \quad (4)$$

where η_d denotes the drive-line efficiency. In figure 4, the driving torque T_w is shown as a function of the wheel rotation speed N_w, for different transmission ratios i and a fixed throttle position α^*.

Furthermore, for each throttle position α^*, the following optimal engine rotation speeds $N_e(\alpha^*)$ can be derived (see figures 5 and 6):

$$N_{e_P}(\alpha^*) = \text{the speed of maximal power (sport mode)} \quad (5)$$

$$N_{e_b}(\alpha^*) = \text{the speed of minimal consumption (economy mode)} \quad (6)$$

The optimal operating lines, corresponding to these different optimal speeds, are shown in figures 2 and 3. Notice that only a CVT can operate along these lines, since continuous shifting is required to track one of them.

To obtain optimal shifting variograms, the curves defined by equations (5)-(6) must be plotted as a function of the vehicle speed. Because of comfort specifications, the optimal paths need to be smoothed. The final variogram for economy mode is shown in figure 7.

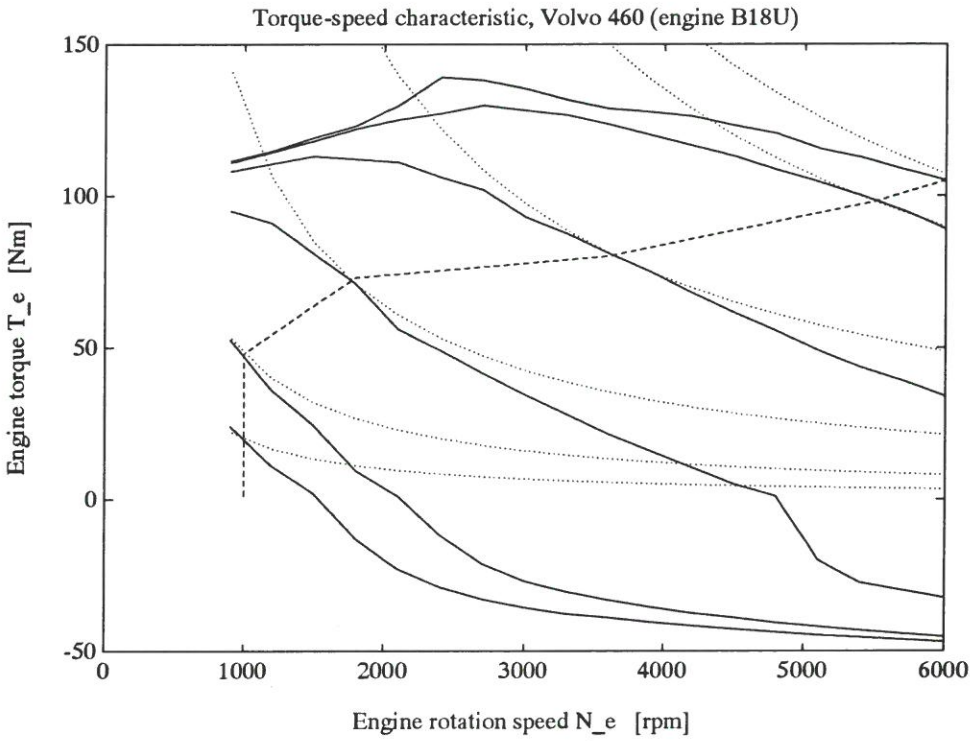


Figure 2: *The experimentally determined torque-speed curves $T_e(N_e)$ for various throttle positions α (full lines): since the engine power must be optimal for sport mode, the optimal operating line for the sport mode (dashed line) is the line through the points where the engine torque curves are tangent to a curve of constant engine power (dotted lines). If this operating line is followed, the power delivered to the wheels will be as high as possible at every time instant: the limits of performance with respect to delivered engine power will be approached.*

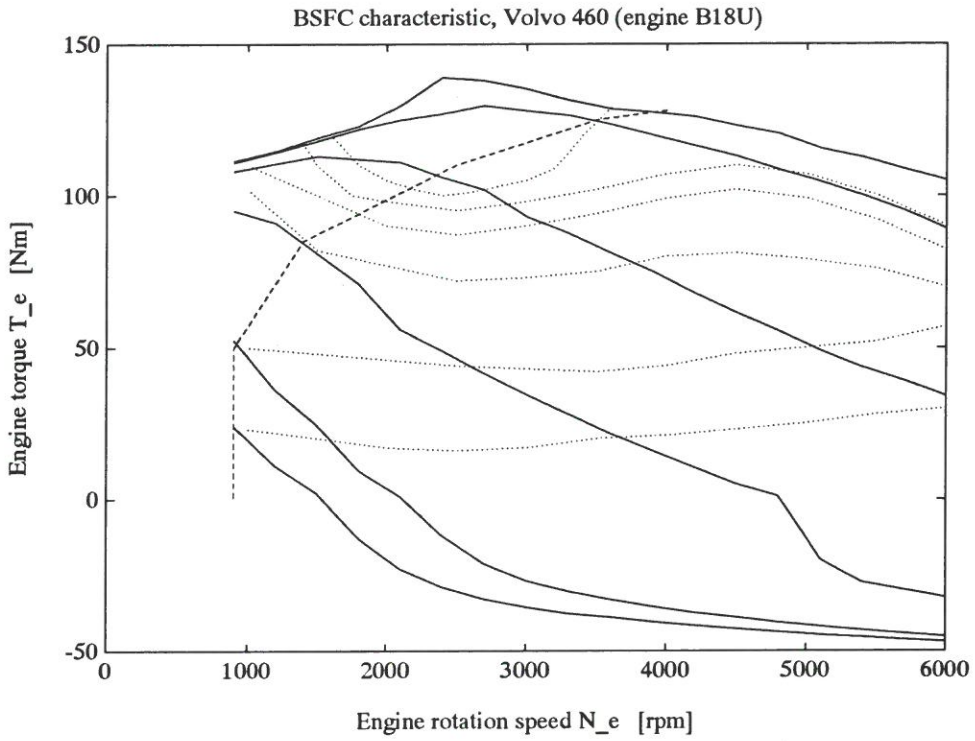


Figure 3: *The BSFC characteristic is obtained by adding lines of constant brake specific fuel consumption (dotted lines) to the torque-speed characteristic. Notice that low brake specific fuel consumption occurs in the upper part of the characteristic. If the optimal operating line for economy mode is followed (dashed line), the brake specific fuel consumption will be small at every time instant: the limits of performance with respect to fuel consumption will be approached.*

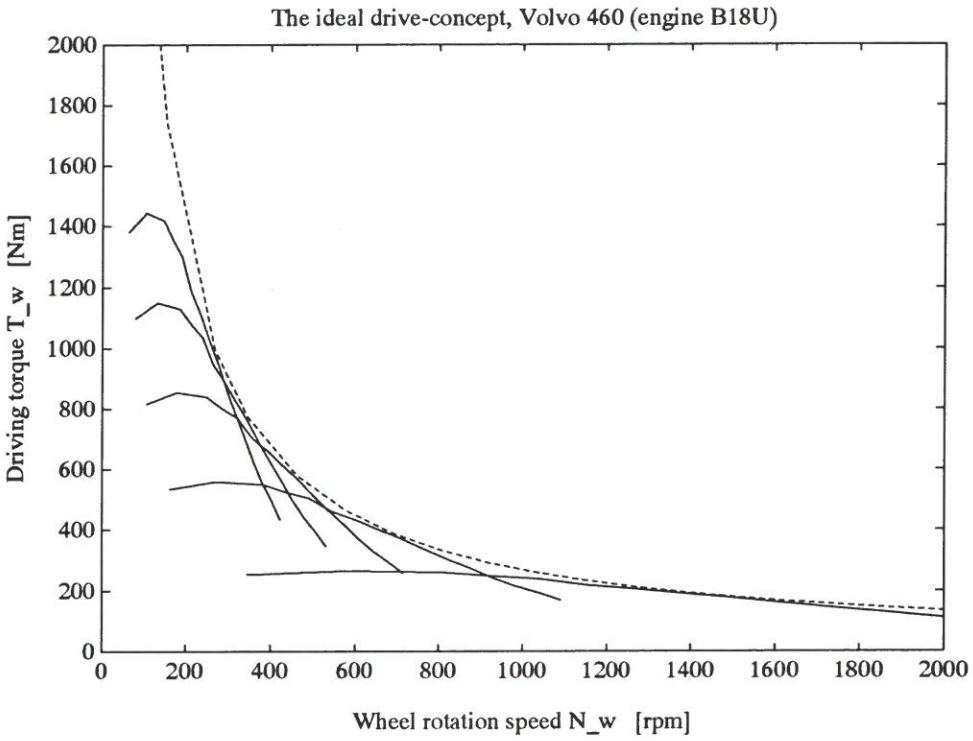


Figure 4: *The driving torque T_w (full lines) as a function of the wheel rotation speed N_w, for different transmission ratios i ($2.6 \leq i \leq 14.2$) and a fixed throttle position $\alpha^* = 35\%$. A drive-line efficiency $\eta_d = 90\%$ is assumed. When the transmission ratio i decreases, the driving torque T_w decreases also. If shifting can be done such that the curve of constant driving power is followed (dashed line), the power delivered to the wheels will be as high as possible at every time instant (sport mode).*

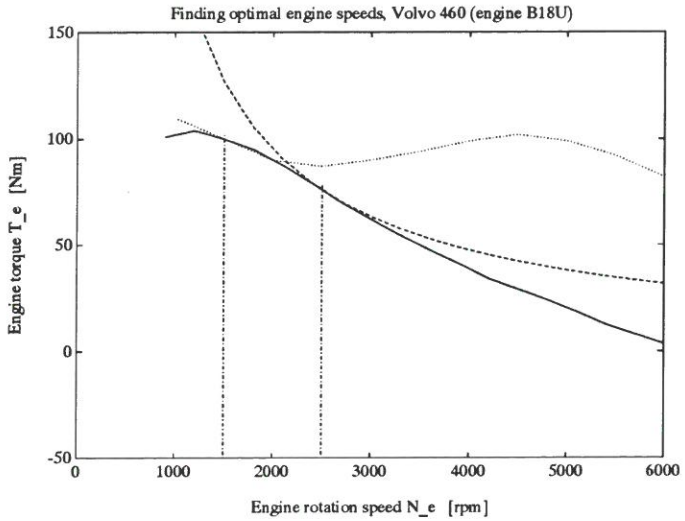


Figure 5: *Deriving the optimal speeds for a throttle position* $\alpha^* = 27.5\%$*:* $N_{e_P}(\alpha^*) = 2500$ rpm *and* $N_{e_b}(\alpha^*) = 1500$ rpm. *Also shown are the torque-speed curve for* $\alpha^* = 27.5\%$ *(full line), a curve of constant brake specific fuel consumption (dotted line) and an hyperbola of constant engine power (dashed line).*

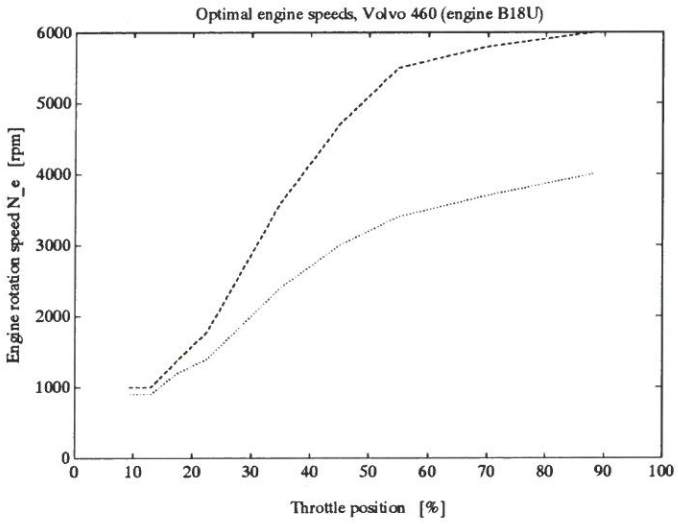


Figure 6: *The optimal speeds* N_{e_P} *(dashed line) and* N_{e_b} *(dotted line) as a function of the throttle position* α*. To realize a compromise between sport mode and economy mode, intermediate curves may be designed.*

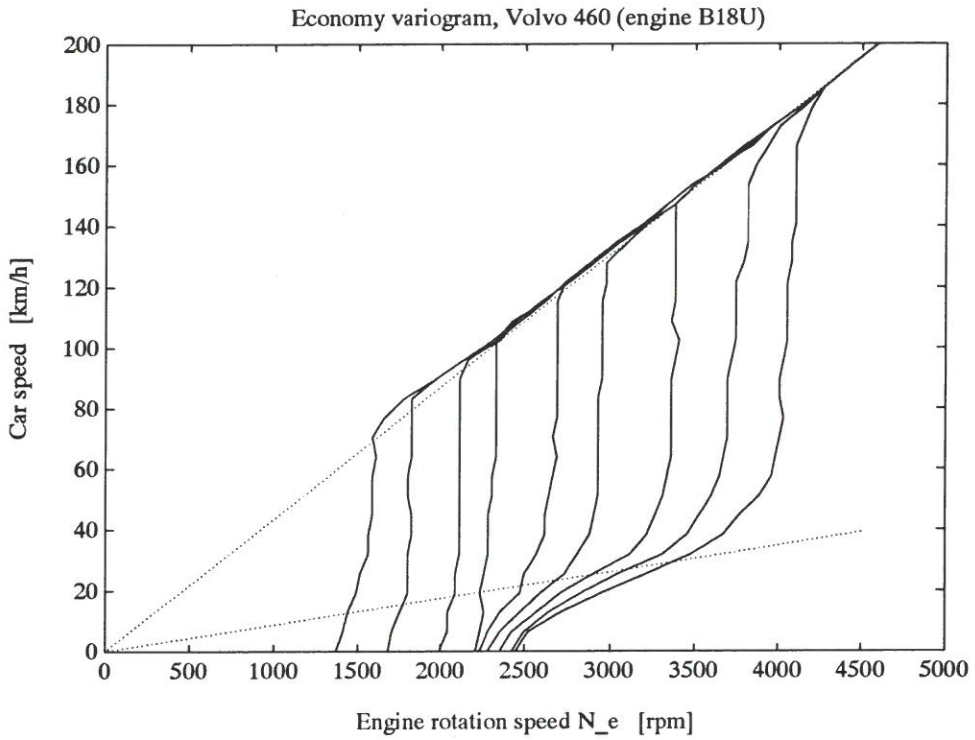


Figure 7: *The economy variogram for a Volvo 460 (engine B18U) with a CVT (full lines). The minimal and maximum transmission ratios are indicated also (dotted lines). To realize an optimal drive-concept, the engine rotation speed must remain constant, at an optimal value that depends on the throttle position (see figure 6). Hence, if the throttle position is fixed, a vertical path between the stall line (car speed equal to zero) and the line of minimal ratio should be followed. However, to meet comfort specifications, these curves need to be smoothed towards the line of maximal ratio. The smoothed sub-optimal shifting paths (for various throttle positions) are shown. Notice that a throttle dependent stall rotation speed is only realizable with an electronically controlled clutch.*

III. POWERTRAIN LEVEL

At the powertrain level, a car with ideal system components is considered. First, an accurate physical model is derived. Next, it is shown how the variogram can be used to implement an optimal drive-concept, to approach the limits of performance of the combustion engine car.

A. Modeling

In the literature, one can find many techniques to model physical dynamic systems. Block diagrams or differential equations are preferred by engineers. However, their major drawbacks are the lack of structure during the model generation phase, the absence of the structure of the physical system in the generated model and the fact that causality problems often arise when subsystems are coupled [6]. Most of these problems originate in the desire of engineers to obtain a computable model. However, this is not the goal of the modeling phase, which is to obtain a true representation of the physical dynamic system. It is known that bond graphs are able to deal with both problems: creating a bond graph gives form to the modeling phase, while analysis of the computational causality of the bond graph will result in a computable model. A detailed description of the bond graph technique and its possibilities is given in [5]. To model the powertrain (see figure 8), a lumped parameter approach as proposed in [3] is used. The powertrain is considered as a system of ideal physical components that are interacting. The final bond graph model is shown in figure 9. Table 1 denotes all components, together with their idealized bond graph elements and bond graph symbols. To handle modeling, simulation and analysis in a powerful manner, the corresponding set of differential and algebraic equations is implemented in the block diagram oriented simulation package Matrix$_X$. Closed-loop simulations are shown in section VI. Although derived for a powertrain with a mechanical CVT, the obtained model can easily be adapted to simulate powertrains that contain a MT, an AT or another type of CVT.

The clutch is modelled as a modulated friction element. The torque T_{cl} that is transmitted through the clutch is given by:

$$T_{cl} = \mu_{cl}(N_e - N_p)Q \tag{7}$$

The friction coefficient μ_{cl} mainly depends on the clutch slip $s = N_e - N_p$, the difference between the engine rotation speed N_e and the primary rotation speed N_p. The signal Q is used to modulate the clutch characteristic. In an electromagnetic powder clutch, Q depends

Component	Bond graph element	Bond graph symbol
Combustion engine	Modulated torque source	$SE(\alpha, N_e)$
Inertia of engine, flywheel, oil pump, clutch shaft and connected clutch parts	Inertance	I_e
Engine-driven gear pump	Modulated resistance	$R_{gp}(N_e, p_s)$
Clutch	Modulated resistance	$R_{cl}(N_e - N_p, Q)$
Inertia of primary shaft, connected clutch parts and primary parts	Inertance	I_p
Variator and final drive reduction	Modulated transformer	$MTF(i_x i_d)$
Equivalent stiffness of secondary shaft, final drive reduction and wheel shafts	Compliance	C_w
Equivalent inertia of secondary parts, secondary shaft, final drive reduction, wheel shafts, wheels and mass of car and passengers	Inertance	I_w
Road load (rol, slope and air resistance)	Modulated resistance	$R_w(N_w)$
Brake	Modulated resistance	$R_b(on/off)$

Table 1: *Bond graph elements and symbols of the different powertrain components.*

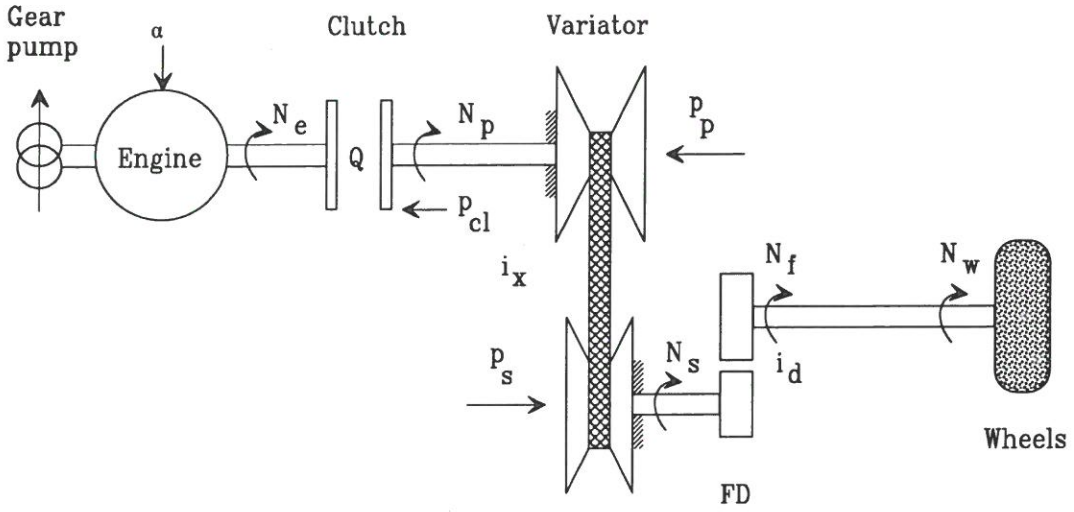


Figure 8: *The powertrain contains a mechanical CVT with a wet multi-plate clutch and a metal pushbelt variator. It's a universal CVT which can be used for all types of vehicles. The variator ratio i_x can be varied by changing the pressures p_p and/or p_s. The clutch control signal Q is determined by the pressure p_{cl}. The operation of the different components is explained in section IV.*

on the exciting current, while in a wet multi-plate clutch, Q is determined by the oil pressure in the clutch piston.

The variator and the final drive reduction are modelled by a single modulated transformer with a variable transformation ratio $i = i_x i_d$. The continuously variable ratio of the variator is indicated by i_x, while i_d is the fixed ratio of the final drive reduction. The ratio i varies between a minimal ratio i_{min} and a maximal ratio i_{max}, which depend on the chosen variator and the final drive reduction. It holds that:

$$N_p = N_f i \tag{8}$$

$$T_p = \frac{T_f}{i} \tag{9}$$

with T_p being the primary torque and T_f the torque that is applied to the wheel shaft. The rotation speed N_f of the wheel shaft at the final drive reduction equals the wheel rotation speed N_w in static situations. If required, the secondary rotation speed N_s can be computed as $N_s = N_f i_d$.

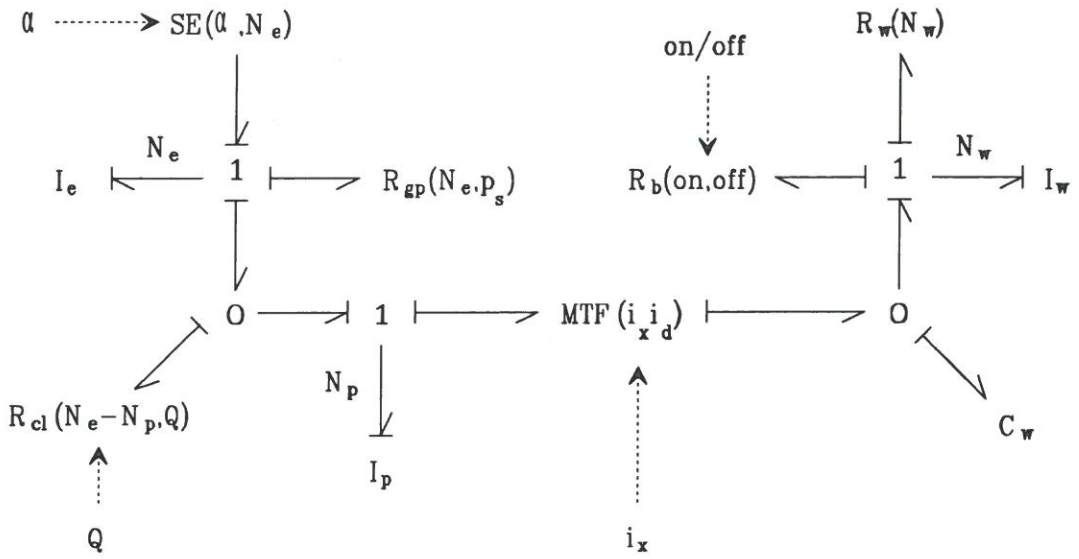


Figure 9: *The causal bond graph of the powertrain in figure 8, to model and compute the interactions between the various inertances, compliances and resistances (see table 1 for a list of symbols and their interpretation). The partial arrows represent power signals, while the dotted arrows show where external signals enter the system. The 1-junctions represent classical force equilibria (Kirchoff's Voltage Law: KVL), while the 0-junctions correspond to speed equilibria (Kirchoff's Current Law: KCL). The causal assignments are indicated by a small causal line on each power signal.*

B. Control design

As shown in section II, the variogram (see figure 7) represents an optimal drive-concept. For a powertrain with a CVT, we propose the control configuration of figure 10. Table 2 summarizes the proposed strategy. The subscript m is used to indicate signals that are *measured.*
During the clutch phase (dotted lines in figure 10 are active), PI_{cl} controls the clutch, to realise the desired shifting traject, while the variator ratio remains constant. Smooth acceleration/deceleration at low vehicle speeds is the major goal. During the variator phase (full lines are active), the variator controller PI_v takes care of variogram tracking. To avoid energy losses, PI_{cl} is now used to keep the clutch slip small. An hysteresis element, driven by the measured clutch slip $s_m = N_{e,m} - N_{p,m}$, is used to generate the reference clutch slip s_{ref}. Smooth switching between both phases is guaranteed if the initial reference clutch slip is well-chosen. This can be seen in the closed-loop simulations in section VI.

Phase	Computation of Q	Computation of i_x
Clutch phase $\frac{N_{p,m}}{N_{w,m}} > i_{max}$	From $N_{e,ref} - N_{e,m}$	Keep $i = \frac{i_{max}}{i_d}$
Variator phase $\frac{N_{p,m}}{N_{w,m}} < i_{max}$	From $s_{ref} - [N_{e,m} - N_{p,m}]$	From $N_{e,ref} - N_{e,m}$

Table 2: *The proposed control strategy for powertrain control. The subscript m is used to indicate signals that are measured.*

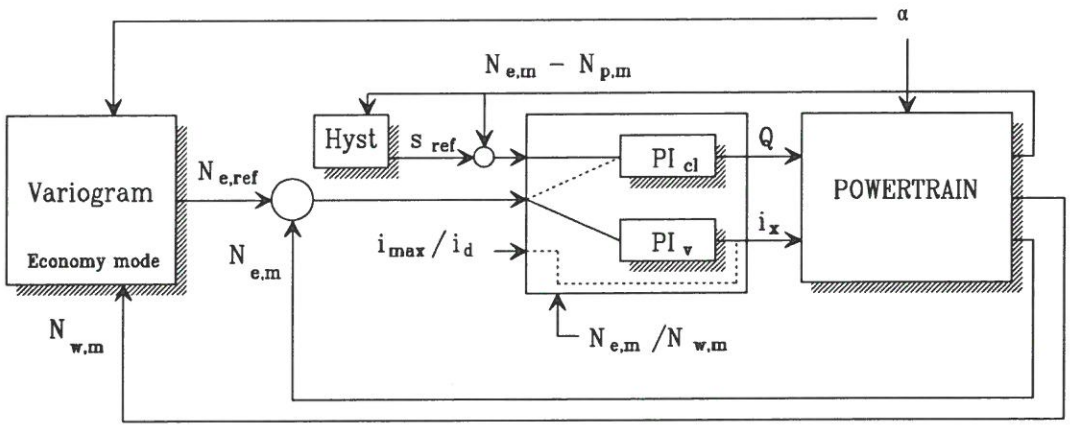


Figure 10: *Variogram control: the reference engine rotation speed $N_{e,ref}$, which is obtained from the measured wheel speed $N_{w,m}$, the measured throttle position α and the desired drive-mode, is compared with the measured engine rotation speed $N_{e,m}$. Two PI-controllers are used to compute the clutch control signal Q and the variator control signal i_x. Trial-and-error, based on closed-loop simulations (see section VI), is used to tune both controllers.*

IV. POWERTRAIN COMPONENT LEVEL

In this section, it is shown how the characteristics of the wet multi-plate clutch and the pushbelt variator can be taken into account. First, reduced static models of both systems are derived. Next, these models are inverted to obtain static feedforward controllers.

A. The wet multi-plate clutch

The wet multi-plate clutch exists of axially slidable friction plates which are connected either to the engine shaft or to the primary shaft by a cottering (see figure 11). A piping in the primary shaft brings oil in the clutch piston. The torque transmitted through the clutch is proportional to the pressure in this piston. The oil is also used for lubrication and cooling of the clutch plates, via small grooves in the plate surfaces [2].

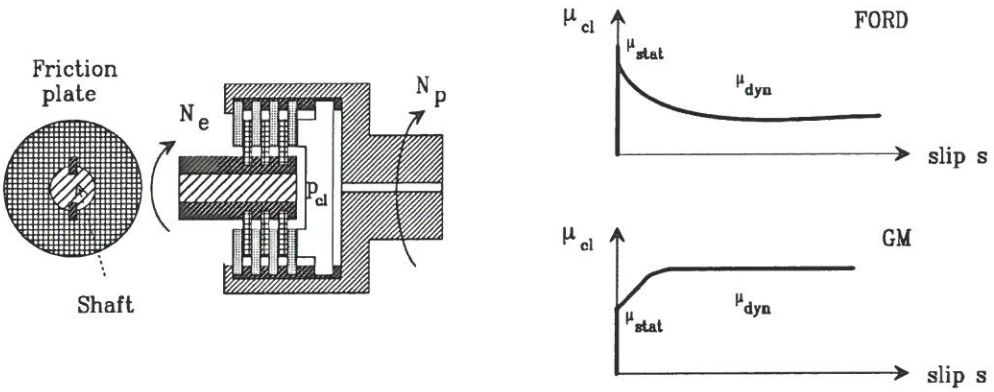


Figure 11: *A cross section and a longitudinal section of the wet multi-plate clutch. For reasons of clarity, only the engine shaft and a connected friction plate are shown in the cross section. For the same reasons, the spring is not shown in the longitudinal section (l). To achieve smooth coupling, the friction coefficient μ_{cl} in wet multi-plate clutches is used as a real design parameter. While Ford asks for $\mu_{dyn} \leq \mu_{stat}$, General Motors asks for $\mu_{dyn} \geq \mu_{stat}$ (r).*

Only a rough static model is derived, because little is known about the exact physical phenomena that take place in the clutch. In fact, too many different (but unknown) phenomena are modelled in a single phenomenon (undermodeling). For a fixed engine rotation speed N_e and primary rotation speed N_p, the clutch equation determines the torque that is transmitted through the clutch:

$$T_{cl} = n\mu_{cl}(N_e - N_p)\left[p_{cl} - \frac{F_0}{A_{cl}}\right] A_{cl} R_m \tag{10}$$

Parameter	Meaning
F_0	preload of the spring
A_{cl}	pressure surface of the clutch piston
R_m	mean friction radius of a plate
n	number of active friction surface pairs

Table 3: *Parameters in the clutch equation.*

with p_{cl} referring to the clutch pressure. Table 3 explains the meaning of the parameters. When no pressure is applied, a spring will open the clutch. Since the plates move only within a very small range and since the spring stiffness is low, the additional spring force is neglected. The friction coefficient μ_{cl} mainly depends on the clutch slip $s = N_e - N_p$ (see figure 11), but also on the type of friction material and on the pattern of the grooves in the plates. From equations (7) and (10), it follows that the clutch control signal Q is determined by:

$$Q = n \left[p_{cl} - \frac{F_0}{A_{cl}} \right] A_{cl} R_m \tag{11}$$

This equation shows that the oil pressure p_{cl} can be used to control the clutch operation. For a desired clutch control signal Q_{ref}, the required clutch pressure p_{cl} can easily be calculated[1]. Closed-loop simulations are shown in section VI.

B. The pushbelt variator

The pushbelt variator (see figure 12) may be considered as the heart of the CVT. The circumferential force of the driving torque T_p at the primary pulley is transmitted by a flexible medium to the secondary pulley. This is however not done by pulling, but by pushing. To do so, a metal belt, existing of strings and links, is used. To obtain flexibility, the links can rotate relatively to each other. Force is transmitted from one link to another, through the line contact of neighbouring links. Strings are used to connect the links. To avoid nodding of the belt, the stress force in the strings must always exceed the pushing force. Compactness, efficiency, a longer life time and the possibility to transmit higher torques are the major advantages of this type of variator [14].

[1] This intermediate step via a non-physical signal Q might look artificial from a control engineer's point of vue. However, it is introduced for didactical reasons and for its attractiveness from a modeling point of view.

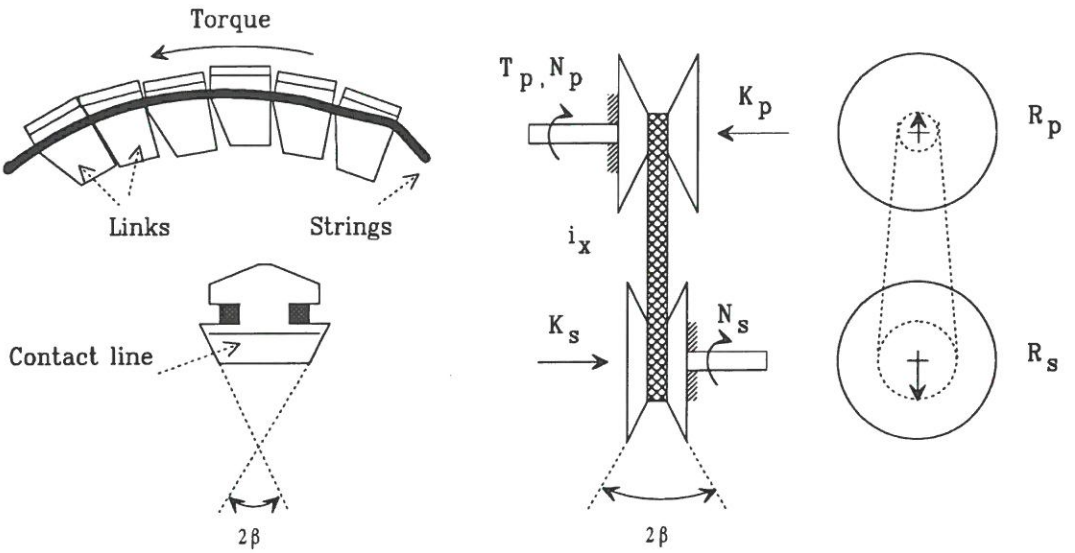


Figure 12: *To transmit power, a pushbelt variator uses a belt that exists of metal links and metal strings. Power is transmitted by pushing, through the line contact of neighbouring links (l). The variator ratio $i_x = R_s/R_p$ can be changed by the pinch forces K_p and/or K_s (r).*

In steady state, the ratio between the secondary radius R_s and the primary radius R_p is equal to the variator ratio i_x. This ratio is adjusted by axial shifting of one of both conical pulley sheaves. Intuitively, one sees that reducing K_p has the same effect as increasing K_s, and vice versa. Therefore, it seems natural to assume that i_x depends mainly on the pinch force ratio K_p/K_s.

From a physical point of view, the belt is a distributed system, so finite element modeling would be required to describe the static and dynamic behavior of the variator. This gives rise to a non-linear model of very high order, that will be useless for control design, unless a model reduction procedure would be applied. But even if such a model could be used, it would be very inaccurate, since too little is known about the exact physical phenomena that occur when the variator is shifting. Therefore, only a static model is derived. Although experiments show that the accuracy varies from time to time and from variator to variator, the model quality is sufficiently high to guarantee a suitable feedforward controller.

For a fixed ratio i_x, it follows from rather involved arguments in [13] that integral equations can be used to compute the static behavior of the variator. In principal, one describes the static equilibrium of the pinch forces K_p and K_s, the belt stresses (determined by the driving torque T_p), the centrifugal forces on the belt mass (determined by the primary rotation speed N_p) and the dry friction between belt and pulleys. By solving these implicit equations in i_x

Parameter	Meaning
A_p	pressure surface of the primary cylinder
A_s	pressure surface of the secondary cylinder
c_p	centrifugal pressure coefficient of the primary cylinder
c_s	centrifugal pressure coefficient of the secondary cylinder
d_s	equivalent stiffness of the secondary spring
$R_{s,0}$	reference radius of the secondary pulley

Table 4: *Parameters in the static equilibria of the pulleys.*

for various values of K_p, K_s, T_p and N_p, it is possible to obtain discrete values of the following multivariate function:

$$i_x = i_x(\frac{K_p}{K_s}, N_p, T_p) \tag{12}$$

Multi-dimensional convex interpolation is used to calculate function values between the discrete points. The static values of the resulting pinch forces K_p and K_s are determined by the static equilibrium at each pulley:

$$K_p = p_p A_p + c_p N_p^2 \tag{13}$$

$$K_s = p_s A_s + c_s N_s^2 + d_s[R_{s,0} - R_s] \tag{14}$$

Table 4 explains the meaning of the used parameters. The rotation speeds N_p and N_s are also related to the radii R_p and R_s by:

$$i_x = \frac{N_p}{N_s} = \frac{R_s}{R_p} \tag{15}$$

Furthermore, for a constant belt length L and a fixed shaft distance d, it holds that:

$$L = 2\sqrt{d^2 + [R_p - R_s]^2} + \pi[R_p + R_s] \tag{16}$$

From equations (13) and (14), it follows that the primary pressure p_p and the secondary pressure p_s can be used as control signals for the variator. To (reach and) hold the desired variator ratio $i_{x,ref}$, equations (12)-(16) can be used to calculate the primary pressure p_p and secondary pressure p_s, since the rotation speeds N_p and N_s are measured and the primary

torque T_p can be estimated from the torque-speed characteristic. However, to avoid the belt from slipping on the pulleys (slipping would destroy the variator), two additional constraints must be taken into account:

$$K_{p,min} = \frac{f_r|T_p|\cos(\beta)}{2\mu_v R_p} \leq K_p \tag{17}$$

$$K_{s,min} = \frac{f_r|T_s|\cos(\beta)}{2\mu_v R_s} \leq K_s \tag{18}$$

Here, a safety factor $f_r \geq 1$ is used. The angle β of the conical sheaves is indicated on figure 12. The dry friction coefficient between the belt and the pulleys is denoted by μ_v.
Equations (12)-(18) can be used to generate the pressures p_p and p_s. Closed-loop simulations are shown in section VI. However, since only static models were considered, additional feedback control is required. Since the final goal is variogram control, it is advised to use the speed error $N_{e,ref} - N_{e,m}$ as input for these feedback controllers. In designing these, one should take care that the constraints (17) and (18) are always satisfied!

V. ACTUATOR LEVEL

As shown in section IV, three hydraulical signals are required to control the wet multi-plate clutch and the pushbelt variator. An electro-hydraulic actuator is used to generate the desired signals. Electronic control is needed to do this in a suitable way. A typical loop with a full explanation of its operation is shown in figure 13. Further results in this section are all related to this loop. Extensions to the other loops can easily be done.

A. Modeling

Bond graph modeling is used to describe the static and dynamic behavior of all hydraulic servo valves in the valve-body. The resulting non-linear dynamic models are implemented as block diagrams in Matrix$_X$.
The bond graph of a model for the secondary valve is shown in figure 14. Table 5 shows the physical phenomena that are taken into account, and the corresponding bond graph elements. For a detailed model description, we refer to [16].
Technical drawings, component information, material characteristics and static and dynamic experiments on a prototype are used to determine the model parameters. As shown in figure 15, the accuracy of the bond graph model is very high, although the high frequency

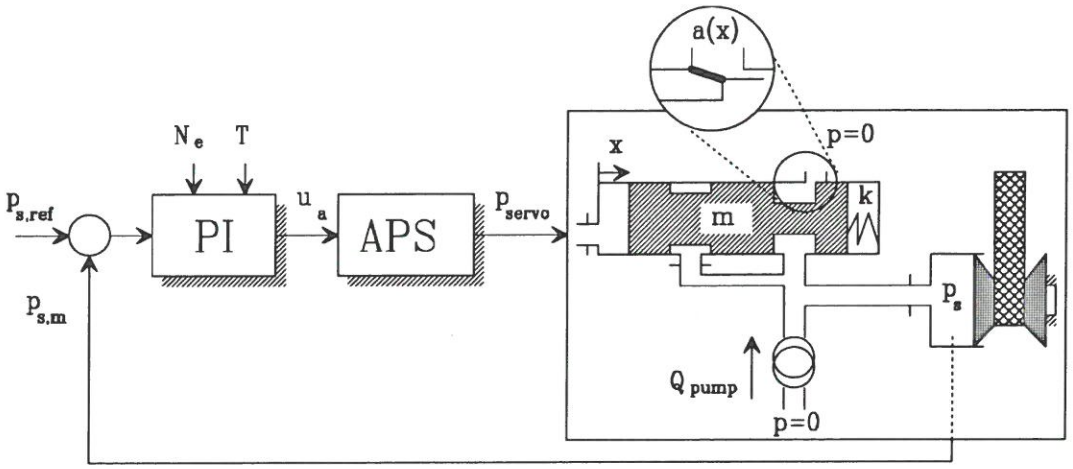


Figure 13: *The secondary circuit of the computer controlled electro-hydraulic actuator: an ideal (assume no gain, no phase) analogue pressure source (APS) drives the non linear hydraulic servo valve (it should be noticed that three way valves in PWM-mode will be used in cars, instead of analogue pressure sources, for reliability and to limit the price of a car with an electronic controlled CVT). The servo pressure p_{servo} determines the desired secondary pressure p_s. If the servo pressure is high, the valve opening $a(x)$ will be large (so the hydraulic resistance is small) and p_s will be small. If the servo pressure is low, the valve opening will be small and p_s will be high. The pump flow Q_{pump} is proportional to the engine speed, since it is delivered by an engine driven gear pump. The oil temperature T and the pump rotation speed N_e are slowly varying disturbances that influence the static and dynamic behavior of the valve. Feedback control is used to reduce their influence on the secondary pressure p_s. Since both disturbances are easily measured, we propose to use an (N_e, T)-scheduled PI-controller.*

components in the simulated pressure are not found in the measured signal. This difference is caused by the fact that pressure measurement is done in a volume at a certain distance from the valve output, while the model calculates the pressure at the valve output. This problem is easily solved by adding an hydraulic low-pass filter (the cylinder and its inlet restriction) to the valve model.

Although extensively used for valve analysis, valve design and control validation, the bond graph models are too complex for control design. In [16], linear system identification (see [8]) is proposed to obtain linear models that can be used for actuator control. An equally distributed servo pressure (noise with a flat spectrum up to 500 Hz, with an amplitude of 2.5 bar) is applied to the bond graph models, to produce identification data, for several fixed engine speeds N_e and fixed oil temperatures T. Within the range of interest (30 bar output pressure),

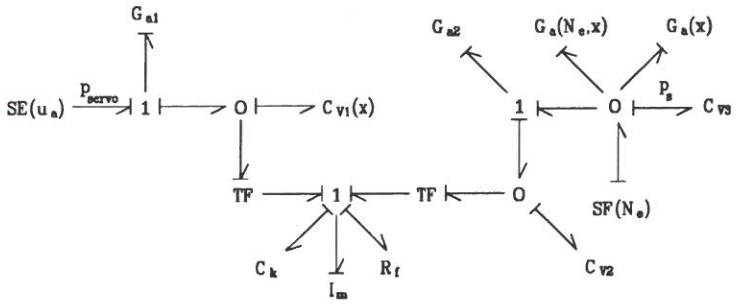


Figure 14: *The bond graph of the secondary valve. Elementary mathematical functions and physical building blocks are combined to implement the system's equations. The 1-junctions represent pressure or force equilibria (KVL), while the 0-junctions correspond to flow equilibria (KCL).*

the dynamics are accurately described by:

$$\frac{p_s(s)}{p_{servo}(s)} = \frac{K(N_e,T)(s - z(N_e,T))}{s^2 + \alpha(N_e,T)s + \beta(N_e,T)} \tag{19}$$

where all parameters are smooth functions of the engine speed N_e and the temperature T.

Phenomenon	Bond graph element
Inertia of the pilot mass m	Inertance I_m
Stiffness of the spring k	Compliance C_k
Viscous friction R on the pilot mass	Resistance R_f
Oil compressibility in a fixed volume V_i	Compliance C_{V_i}
Oil compressibility in a varying volume $V_j(x)$	Modulated compliance $C_{V_j}(x)$
Damping of a fixed orifice a_i	Conductance G_{a_i}
Damping of a varying orifice $a(x)$	Modulated conductance $G_a(x)$
Jet stream effects around $a(x)$	Modulated conductance $G_a(N_e, x)$
Engine driven gear pump	Modulated flow source $SF(N_e)$
Analogue pressure source (APS)	Modulated pressure source $SE(u_a)$

Table 5: *Physical phenomena in the secondary circuit. For reasons of confidentiality, numerical model parameters can't be mentioned here.*

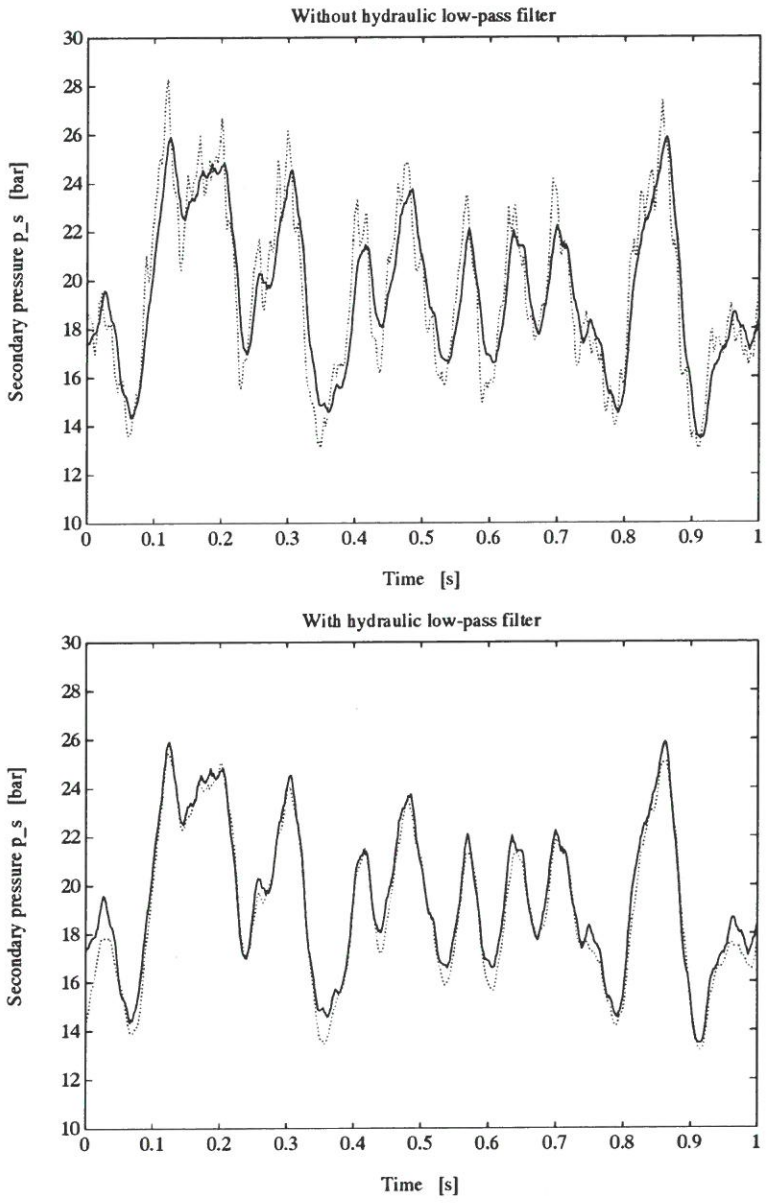


Figure 15: *The measured (full line) and the simulated secondary pressure (dotted line) almost coincide. The parameters of the model are adjusted to the prototype's parameters (t). If an hydraulic low-pass filter is added, the accuracy of the model prediction is even better (b).*

Measure	Specification
Steady state error e_{ss} (bar)	$e_{ss} = 0$
Settling time T_s (s)	$T_s \leq 0.080$
Overshoot os (%)	$os = 0$
Phase margin pm (°)	$pm \geq 25$
Gain margin gm (dB)	$gm \geq 2$
Actuator signal u_a (Volt)	$0 \leq u_a \leq 4$

Table 6: *Closed-loop specifications of the electronically controlled secondary circuit, for a polynomial reference input with a height of* 15 *bar. A high static and dynamic accuracy* ($e_{ss} = 0$, $T_s \leq 0.080$) *and no overshoot* ($os = 0$) *are required to prevent the belt from slipping on the pulleys. To deal with model errors and parameter uncertainties, the phase margin and the gain margin must be high* ($pm \geq 25$, $gm \geq 2$). *Since the supply pressure of the servo valves (APS) is limited to* 4 *bar, the actuator signal must be restricted also* ($0 \leq u_a \leq 4$).

B. Control design

The basic function of an actuator is to transform the corrective signal delivered by the controller into an input for the controlled system. In the ideal case, the actuator will not influence the transformation, but in practice, it turns out that the static and dynamic characteristics of the actuator itself must be taken into account. To minimize this influence and to guarantee that the remaining influence is the same under all circumstances, actuator control is often implemented. In our case, the speed and temperature dependency of the valve-body pressures is the main reason for doing actuator control. Although static feedforward signals can be computed from the bond graph equations, additional feedback is required to deal with uncertainties. Here, we will only use feedback control.
The design specifications are given in table 6. The following equations are used to tune the PI-controller in a set of operating points:

$$K_p(N_e,T) = \left[\frac{0.9}{R(N_e,T)L(N_e,T)}\right] p_f(N_e,T) \quad (20)$$

$$T_i(N_e,T) = [3.3L(N_e,T)]\, i_f(N_e,T) \quad (21)$$

A precise definition of the reaction rate R and the lag L is given in [4]. For a second order system, $R(N_e,T)$ and $L(N_e,T)$ can be calculated analytically. Notice that if the factors

$p_f(N_e, T)$ and $i_f(N_e, T)$ are equal to one, the classical step response tuning method of Ziegler-Nichols is obtained [17]. However, to meet all design specifications, the factors $p_f(N_e, T)$ and $i_f(N_e, T)$ are introduced. In practice, they are smooth functions of the speed N_e and the oil temperature T. On-line interpolation in the (K_p, T_i) space is used to compute the controller parameters in the actual (measured) operating point $(N_{e,m}, T_m)$.
It is shown in [16] that a well-tuned (N_e, T)-scheduled PI-controller is able to guarantee robust performance over a wide range of operation (20 °C $\leq T \leq$ 90 °C, 1500 rpm $\leq N_e \leq$ 4500 rpm). Random checks show that the design specifications are met in every operating point. It is tacitly assumed that the specifications are also met if the engine rotation speed N_e and the oil temperature T vary slowly.

VI. COMBINED RESULTS

Models and controllers for the different (sub)systems were derived in sections III, IV and V. In this section, these models and controllers are combined, to obtain a single hierarchical model and a single hierarchical controller. Closed-loop simulations demonstrate that the proposed model based approach works satisfactorily.

A. Topdown modeling

The final result of the topdown modeling approach is a highly non linear multiple input multiple output model with a hierarchical structure (see figure 16):

- Model M_1 describes the interactions between the several powertrain components, the car and the car environment (see figure 8).
- Model $M_{2,\mathrm{cl}}$ describes the clutch (see figure 11), while model $M_{2,\mathrm{v}}$ is used to describe the variator (see figure 12).
- Model M_3 describes the behavior of the various hydraulic servo valves and their interactions (see figure 13 for the secondary circuit).

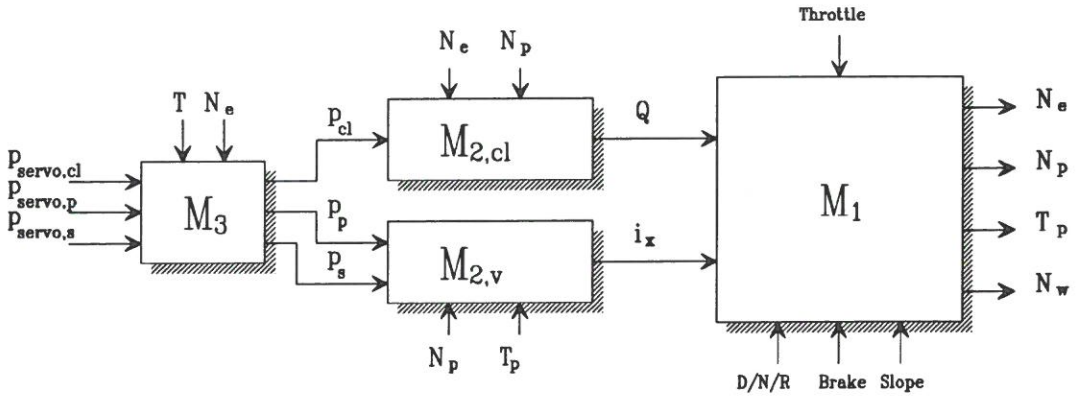


Figure 16: *The final hierarchical model. Inputs are the servo pressures $p_{servo,cl}$, $p_{servo,p}$ and $p_{servo,s}$, the oil temperature T, the throttle position α, the drive sense (D/N/R), the brake signal and the slope of the road. Computed outputs are the rotation speeds N_e, N_p and N_s, the primary torque T_p and the actuator pressures p_{cl}, p_p and p_s.*

B. Hierarchical control

The models of the different subsystems are used for initial tuning of a feedforward controller and several feedback controllers. Further fine-tuning of the hierarchical controller (see figure 17) must be done on a real test setup.

- To realize variogram control, the feedback controller C_1 is used (see table 2 and figure 10). The powertrain model M_1 is used to tune this controller.
- The clutch model $M_{2,\mathrm{cl}}$ (see equation (11)) is used to calculate the feedforward controller $C_{2\mathrm{ff,cl}}$.
- From the variator model $M_{2,\mathrm{v}}$, a static feedforward controller $C_{2\mathrm{ff,v}}$ is easily determined (see equations (12)-(18)). To deal with model uncertainties, a feedback controller $C_{2\mathrm{fb,v}}$ may be added. This controller can be tuned using M_1 and $M_{2,\mathrm{v}}$. Although not implemented now, we keep it as an additional degree of freedom for the control system of the test setup.
- Based on linearized versions of the valve-body model M_3, feedback controllers C_3 for the actuator are determined (for the secondary circuit, equation (19) defines a linearized model, while equations (20) and (21) indicate how the corresponding PI-controller can be tuned).

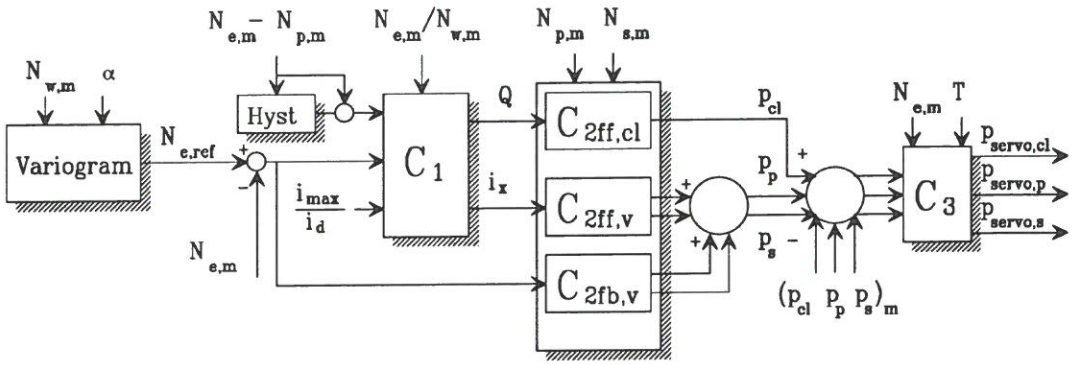


Figure 17: *The proposed hierarchical controller: besides the calculations in the subcontrollers, multi-dimensional convex interpolation in the engine characteristic table, the variogram table and the table of controller parameters is required.*

C. Closed-loop simulations

For reasons of confidentiality, specific numerical model parameters and controller parameters can't be mentioned here. Closed-loop simulations of realistic driving situations demonstrate that the proposed control scheme works well (on simulation). Whether it will also do in practice, will be tested experimentally in the near future[2].

The applied throttle signal and the slope of the road are shown in figure 18. An optimal drive-concept is guaranteed by variogram control (see figures 19 and 20). The feedback controller C_1 computes the clutch control signal Q and the variator control signal i_x (see figure 21). The hydraulical signals p_{cl}, p_p and p_s that are required to realize Q and i_x are computed by the feedforward controllers $C_{2\text{ff,cl}}$ and $C_{2\text{ff,v}}$ (see figure 22). The electro-hydraulical actuator is assumed to be ideal. Results from actuator control (see figure 23 for control of the secondary circuit) show that this assumption is valid if the controller C_3 is well-tuned.

[2]We recognize that the implementation of the proposed control scheme might be hampered by a lot of practical problems: how should we select our sampling rate(s)? Can we deal with measurement noise? How sensitive is the overall control design for uncertainties? Is the algorithm implementable in a car's simple control system, or must it be simplified? To find out what problems will occur, we are actually configuring a laboratory setup and a test car.

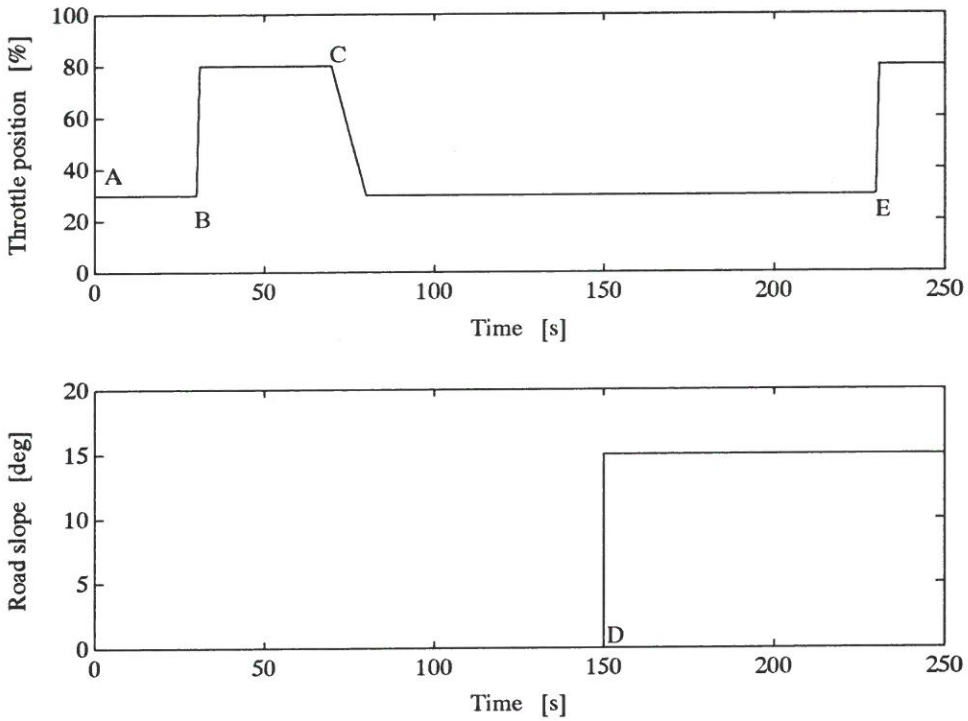


Figure 18: *The car starts from stall: the throttle signal is* 30% *and the brake is active (on). At time* $t = 0$ s *(event A), the brake is set free (off), while the throttle signal remains constant* (30%). *At time* $t = 30$ s, *a kickdown to* 80% *occurs (event B). At time* $t = 70$ s, *the throttle signal decreases rather slowly* (8.3%/s) *to* 30% *(event C). At time* $t = 150$ s, *the slope of the road changes from* 0 *to* 15 $^\circ$ *(event D). At time* $t = 230$ s, *a new kickdown to* 80% *occurs (event E).*

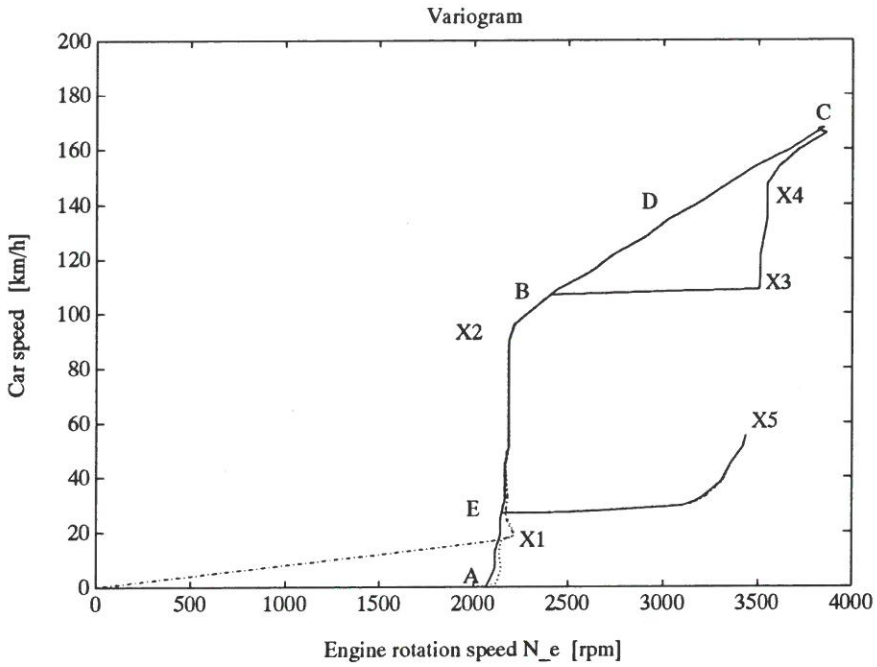


Figure 19: *The desired variogram (full line) and the realized variogram, obtained by plotting the car speed versus the engine rotation speed (dotted line). The dashdotted line represents the evolution of the primary speed N_p as a function of the car speed. Initially, the wet multi-plate clutch is open ($N_e - N_p = 2000$ rpm) and the variator ratio i_x is maximal. Once the brake is set free (event A), the clutch slip decreases fast to a small value (C_1 operates in clutch phase). At a car speed of 15 km/h, the clutch is locked (event X1) and the pushbelt variator shifts slowly (C_1 starts to operate in variator phase). It should be noticed that the engine rotation speed N_e remains almost constant ($N_e \approx 2200$ rpm), while the car speed increases. When the minimal variator ratio is reached (event X2), the engine rotation speed and the car speed remain proportional. When the first kickdown occurs (event B), the variator shifts down fast: the car speed remains 110 km/h, while the engine rotation speed changes from 2500 rpm to 3500 rpm. Once the ideal engine rotation speed is reached (event X3), the variator shifts up slowly, till the minimal ratio is reached again (event X4). Further acceleration to a stationary point (80%, 170 km/h) is done with this fixed minimal variator ratio. When the throttle position decreases (event C), the car decelerates to another stationary point (30%, 140 km/h), without shifting. However, when the road slope changes (event D), the variator slowly shifts down, till a new stationary point is reached (30%, 30km/h). When the second kickdown occurs (event E), the variator shifts again, to realize the corresponding optimal engine rotation speed of 3500 rpm (event X5).*

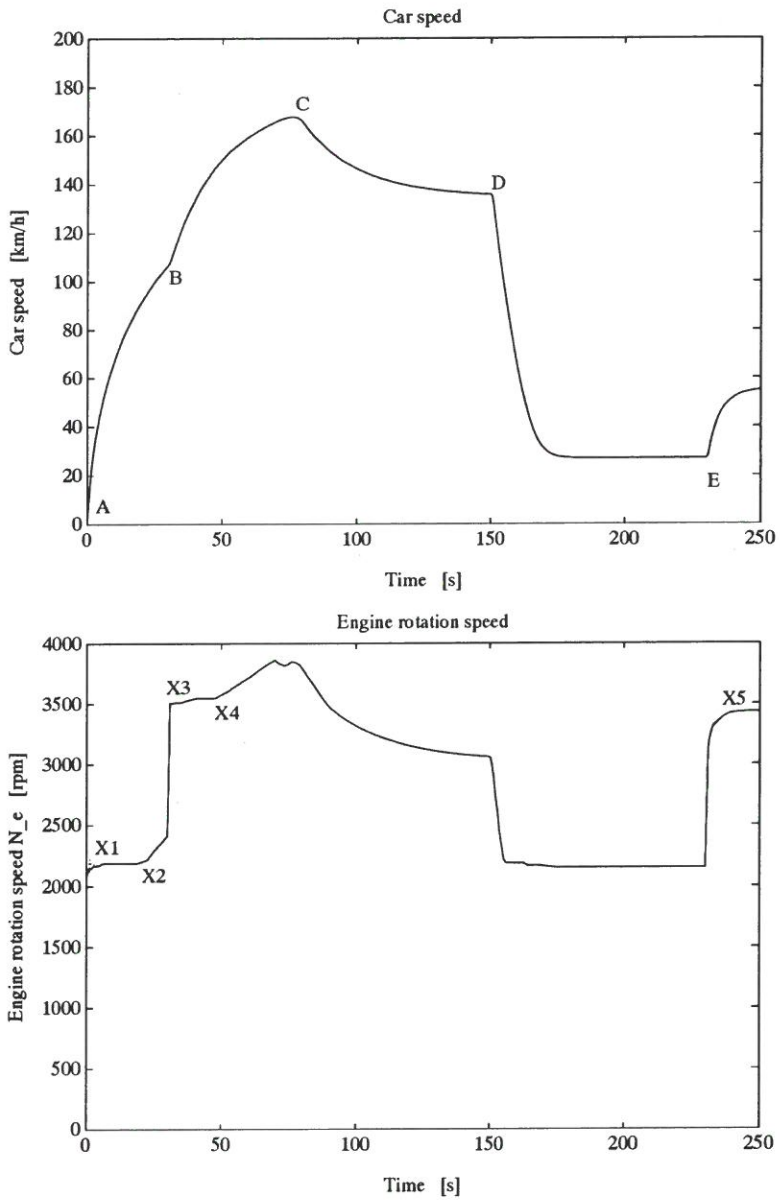


Figure 20: *The car speed (t) and the engine rotation speed N_e (b).*

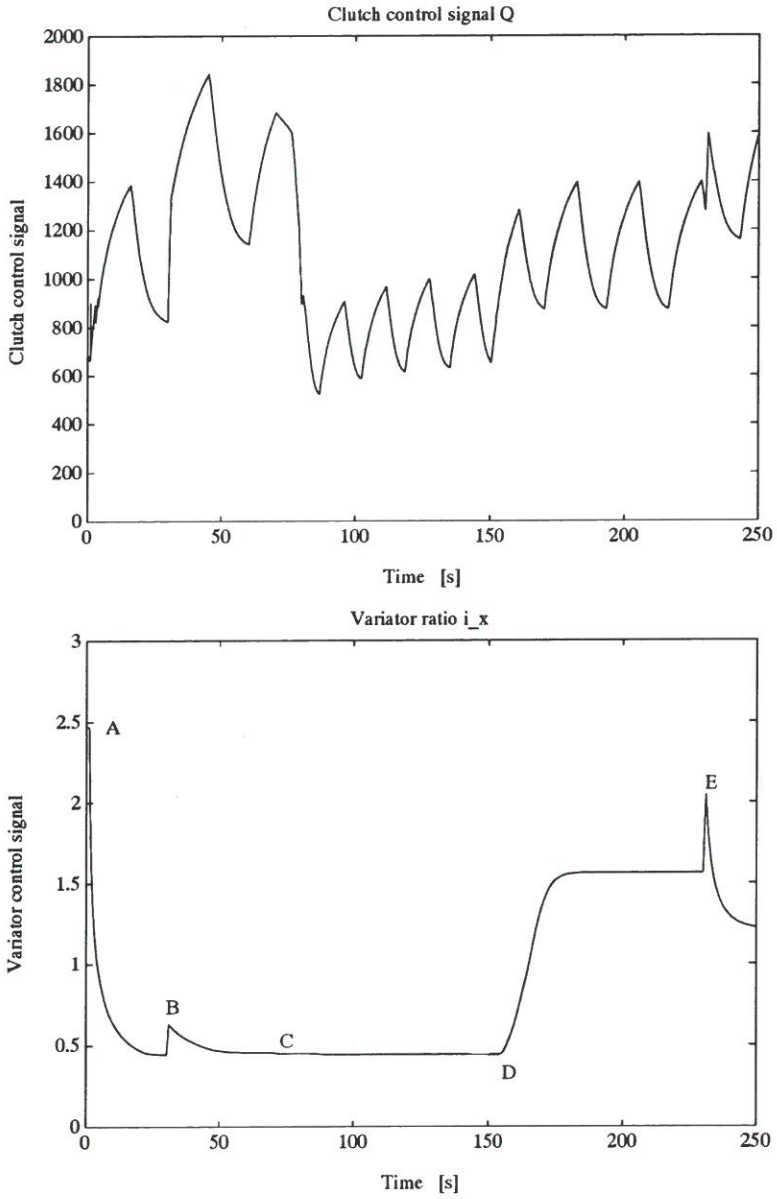


Figure 21: *The clutch control signal Q oscillates, since the hysteresis block (see figure 10) is active during the variator phase (t). The variator shifts continuously between a minimal and a maximal ratio (b).*

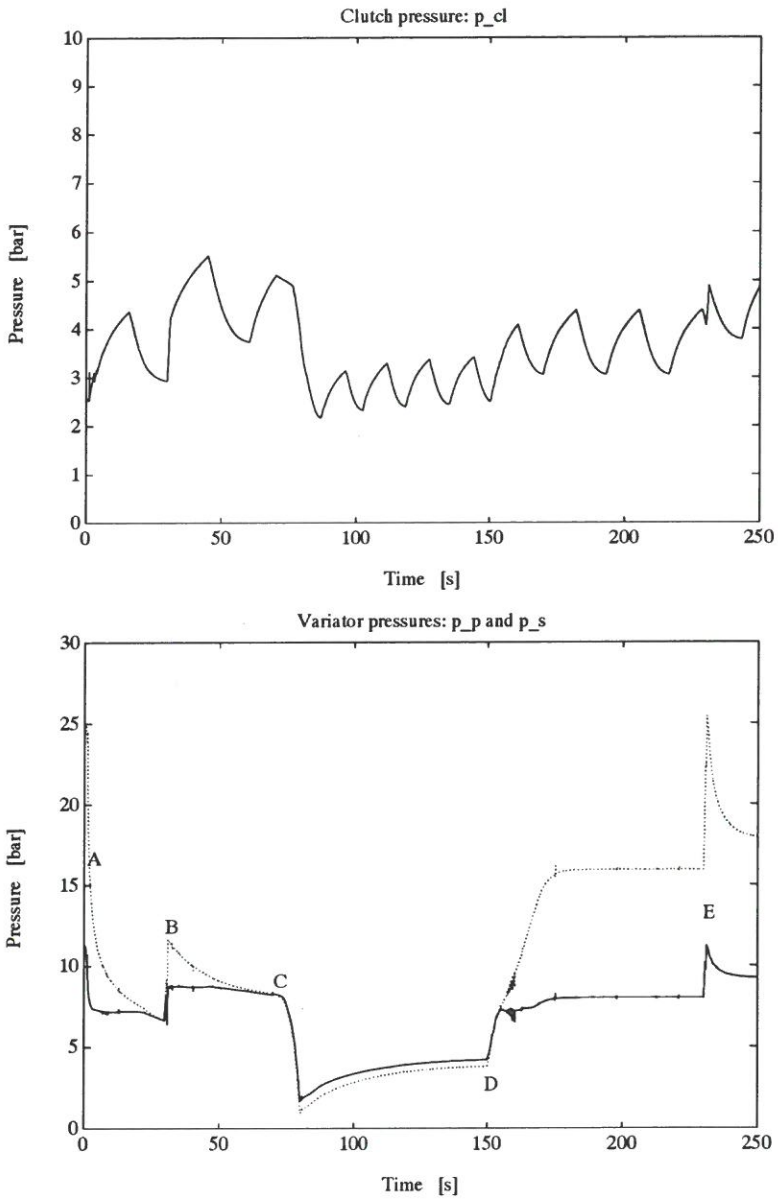


Figure 22: *Since the clutch slip s, the engine torque T_e and the primary rotation speed N_p are measured, the static models $M_{2,\mathrm{cl}}$ and $M_{2,\mathrm{v}}$ can be used to calculate the feedforward signals. The applied clutch pressure p_{cl} must oscillate, since the hysteresis block is active in the variator phase (t). The oscillations (around time $t = 160$ s) in the applied primary pressure p_p (full line) and the applied secondary pressure p_s (dotted line) must be neglected, because they are introduced by the simulation software (b).*

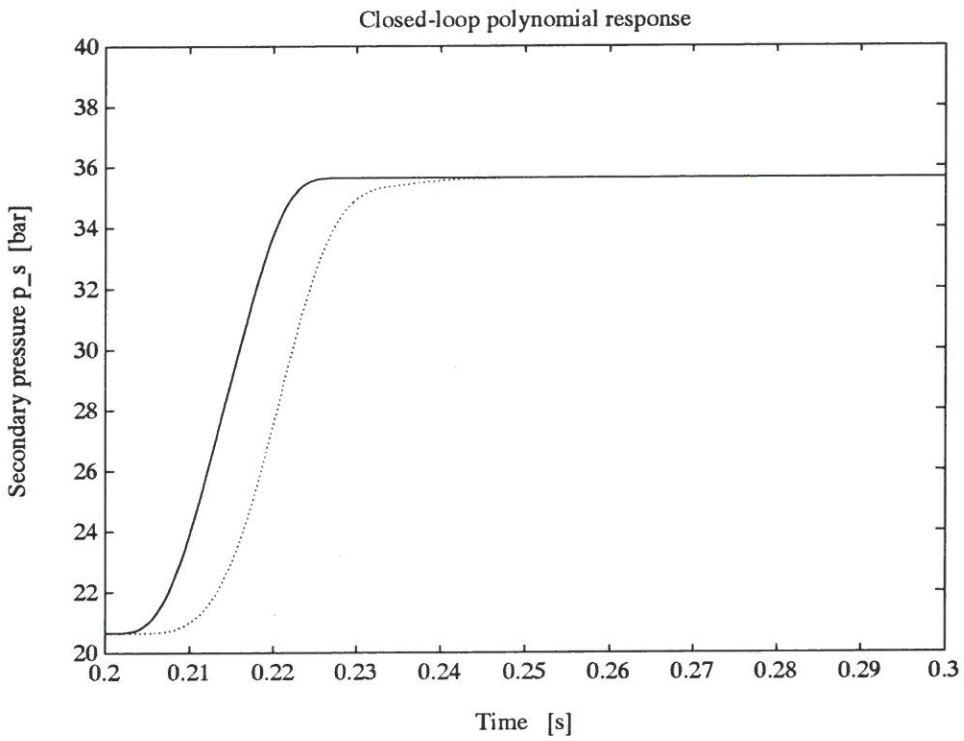


Figure 23: *The closed-loop response (dotted line) of the secondary circuit, for a polynomial reference input with a height of* 15 *bar (full line), an oil temperature* $T = 67\ ^{\circ}\mathrm{C}$ *and a pump rotation speed* $N_e = 3500$ rpm. *With* $K_p = -0.017566$ *and* $T_i = 0.001117$, *all specifications are satisfied* ($e_{ss} = 0$, $T_s = 0.0449$, $os = 0\%$, $pm = 79$, $gm = 3.6$ *and* $0.4 \leq u_a \leq 2$). *Extensive random checking shows that the specifications are met for all possible pairs* (N_e, T). *This demonstrates that the actuator may be assumed to be ideal, if actuator control is implemented when doing powertrain control.*

VII. CONCLUSIONS

A mechatronics approach is used to tackle the powertrain control problem of combustion engine cars. It is shown that, due to the engine characteristics, an optimal drive-concept can only be realized with a CVT. Using computer control, it is possible to approach the limits of performance of combustion engine cars.
In this paper, we presented a model based approach for electronic control of a CVT with a wet multi-plate clutch and a pushbelt variator. A topdown approach is proposed to translate the powertrain control problem into a set of hierarchically related subproblems. Bond graph modeling, static modeling and linear identification are used to obtain models of the powertrain, the wet multi-plate clutch, the pushbelt variator and the electro-hydraulic actuator. Once the static and/or dynamic behavior of all components and their interactions are modelled, these models are easily implemented in Matrix$_X$ [10]. Based on these models, Computer Aided Control System Design (CACSD) methods are used to design controllers for all subsystems. Closed-loop simulations have demonstrated that the proposed model based approach works well.

To further improve the closed-loop performance, more theoretical research is required: are other modeling techniques able to generate better models? Does it make sense to search for exact dynamic models of the clutch and the variator? Can dynamic feedforward improve the performance? Can we apply observer-based or optimization based control? What are the possibilities of neural control and fuzzy control?
Is there an advantage (improved performance), or only a price (increased complexity) to be paid?

To conclude, let us state that electronic control of a CVT opens new perspectives for powertrain control of combustion engine cars. For the first time, the transmission is the active element in the loop: the engine is only a power source, that delivers power as commanded by the transmission.

REFERENCES

[1] Aström K.J. and Wittenmark B., *Computer Controlled Systems*, Englewood Cliffs, Prentice Hall, New York, 1984.

[2] *Borg-Warner Automotive Friction Products*, Borg-Warner Automotive, 1991.

[3] Dransfield P., *Hydraulic control systems. Design and analysis of their dynamics*, Springer-Verlag, New York, 1981.

[4] Franklin G.F. and Powell J.D., *Digital control of dynamic systems*, Addison-Wesley, New York, 1980.

[5] Karnopp D.C. and Rosenberg R.C., *System dynamics: a unified approach*, Wiley & Sons, New York, 1975.

[6] Karnopp D.C., *Structure in dynamic system models: why a bond graph is more informative than its equations*, IMACS Trans. on Scientific Computation-88, Vol. 3: modeling and simulation of systems. (Ed. P.C. Breedveld *et al*), pp. 15-18, J.C. Balzer AG, Basel, 1989.

[7] Leising M.B., Benford H. and Holbrook G.L., *The all-adaptive controls for the Chrysler Ultradrive Transaxle*, SAE 890529, 1989.

[8] Ljung L., *System identification: theory for the user*, Prentice-Hall, Englewood Cliffs, New Jersey, 1987.

[9] Matlab, *Matlab for Unix Computers, User's Guide*, The Mathworks Inc., Cochituate Place, 24 Prime Park Way, South Natick, MA 01760.

[10] Matrix$_X$, *Reference Manual and System Build*, Integrated Systems Inc., 2500 Mission College Boulevard, Santa Clara, California.

[11] Minten W., Vanvuchelen P. and De Moor B., *Modeling of an electronically controlled continuously variable transmission*, Proc. of the International Conference on Bond Graph modeling, pp. 223-228, La Jolla, California, 1993.

[12] Narumi N., Suzuki H. and Sakakiyama R., *Trends of powertrain control*, SAE 901154, 1990.

[13] Schaerlaeckens W. and Van Rooij J., *De metalen V-band, een theoretische benadering: algemene krachtenbeschouwing - het krachtenspel - de energetische verliezen in duwband en CVT*, Mechanische Technologie, pp. 14-19, pp. 21-26, pp. 22-27, February, March, April 1992, in Dutch.

[14] Mom G. and Scheffers H., *De Nieuwe Steinbuch, de complexe aandrijflijn, deel 3B*, Kluwer Technische Boeken BV, Antwerpen, 1993, in Dutch.

[15] Vanvuchelen P., De Moor B. *et al*, *Modeling, analysis, design and control of an electronically controlled continuously variable transmission (1-6)*, Collected master's theses, ESAT, Dept. of Electrical Engineering, Katholieke Universiteit Leuven, Leuven, 1990-1993, in Dutch.

[16] Vanvuchelen P. and De Moor B., *Modeling, analysis, design and control of electro-hydraulic servo systems: bridging the gap between theory and practice*, ESAT-SISTA report 1993-37, ESAT, Dept. of Electrical Engineering, Katholieke Universiteit Leuven, Leuven, August 1993. Submitted for publication.

[17] Ziegler J. and Nichols N., *Optimum settings for automatic controllers*, Transactions on the A.S.M.E., no. 64, pp. 759-768, 1942.

APPENDIX A

Nowadays, there exists no excellent integrated software dealing with modeling, simulation, identification, analysis and design together. Bond graph pre-processor types like CAMP have the disadvantage that the syntaxis of ACSL must be known, in order to edit the processed bond graph for non-linearities. On the other hand, bond graph simulators like CAMAS don't have these drawbacks, but the analysis of the constructed models is not yet supported. Only programs like Matrix$_X$ or Matlab [9] provide integrated tools to solve our problems. But since the input file must consist of (causal) block diagrams or alike structures, conversion from the bond graph models to block diagrams is required.
Because the graphical input capabilities and the hierarchical library structure of Matrix$_X$ were superior to Matlab, the former is used as the software tool for simulation, identification, analysis and design. The use of so called superblock structures (Matrix$_X$ has nice capabilities to construct structured or nested block diagrams) reflects very well the idea of top-down modeling. Figure 16 represents the major substructures in the library.

- At the bottom level, models of the different physical phenomena in the actuator are generated. One level higher, these models are used to construct the models of the different servo valves. Those two levels deal with the actuator design phase, taking into account the physical behavior of the actuator. Structural design and physical parameter optimization are the main objectives here. Furthermore, these models are used to generate I/O-data for linear system identification. The parameters of the identified models are stored in multi-dimensional interpolation tables, that can easily be used in

block diagrams. These linearized models are used for control design. Several control laws are implemented as parametrized superblocks. Control parameter optimization is the main objective.

- At the third level, the static models of the wet multi-plate clutch and the pushbelt variator are constructed. The clutch is modelled by equation 11. The experimentally determined friction coefficient $\mu_{cl}(N_e - N_p)$ is modelled by a fitted function (in our case, a sum of exponentials). As a model for the variator, we use again a multi-dimensional interpolation table (see equation 12).

- At the top level, the model of the powertrain is constructed. To model the combustion engine, the torque-speed characteristics (see figure 2) are stored in a multi-dimensional interpolation table. Models of the gear pump, the road load and the brake are implemented as analytical function blocks, whose structures and parameters are determined experimentally.

At every level, physical phenomena are modelled. To guarantee that the physical parameters of the model correspond to the physical parameters of the prototype, multiple static and dynamic experiments were carried out. Software for curve fitting, equation solving and parameter optimization was used to determine approximate functions and/or parameters.

APPENDIX B

This appendix contains a list of the most important notations that are used through the paper.

- α : throttle position (%)
- b_e : brake specific fuel consumption (g/kWh)
- i : transmission ratio
- i_d : ratio of the final drive reduction
- i_x : ratio of the variator
- i_{min} : minimal transmission ratio
- i_{max} : maximal transmission ratio

- K_p : pinch force on the primary pulley (N)
- K_s : pinch force on the secondary pulley (N)
- N_e : engine rotation speed (rpm)
- N_f : rotation speed behind the final drive reduction (rpm)
- N_p : rotation speed of the primary pulley (rpm)
- N_s : rotation speed of the secondary pulley (rpm)
- N_w : rotation speed of the wheels (rpm)
- N_{e_P} : rotation speed of maximal power (rpm)
- N_{e_b} : rotation speed of minimal consumption (rpm)
- P_e : delivered engine power (W)
- P_m : driving power at the wheels (W)
- p_{cl} : clutch pressure (bar)
- p_p : primary pressure (bar)
- p_s : secondary pressure (bar)
- $p_{cl,servo}$: clutch servo pressure (bar)
- $p_{p,servo}$: primary servo pressure (bar)
- $p_{s,servo}$: secondary servo pressure (bar)
- Q : clutch control signal (Nm)
- s : clutch slip (rpm)
- T : oil temperature $(°C)$
- T_{cl} : torque transmitted through the clutch (Nm)
- T_e : delivered engine torque (Nm)
- T_f : torque applied to the wheel shaft (Nm)

- T_p : torque on the primary pulley (Nm)
- T_s : torque on the secondary pulley (Nm)
- T_w : driving torque at the wheels (Nm)